Research Article

For reprint orders, please contact: reprints@futuremedicine.com

Epigenomics

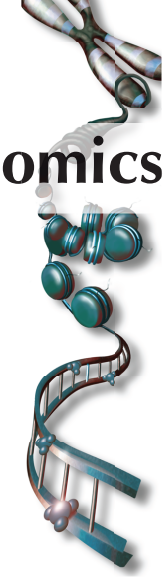

m^{6}A RNA modification modulates gene expression and cancer-related pathways in clear cell renal cell carcinoma

Yimeng Chen[1], Cuixing Zhou[1], Yangyang Sun[1], Xiaozhou He**,[1] & Dong Xue*,[1]

[1]Department of Urology, The Third Affiliated Hospital of Soochow University, Changzhou 213003, Jiangsu, China

*Author for correspondence: Tel.: +86 135 8530 4321; xuedongdx@163.com

**Author for correspondence: czyyhxz@sina.com

Aim: To systematically profile the global m^{6}A modification pattern in clear cell renal cell carcinoma (ccRCC). **Methods:** m^{6}A modification patterns in ccRCC and normal tissues were described via m^{6}A sequencing and RNA sequencing, followed by bioinformatics analysis. m^{6}A-related RNAs were immunoprecipitated and validated by quantitative real-time PCR (qPCR). **Results:** In total, 6919 new m^{6}A peaks appeared with the disappearance of 5020 peaks in ccRCC samples. The unique m^{6}A-related genes in ccRCC were associated with cancer-related pathways. We identified differentially expressed mRNA transcripts with hyper-methylated or hypo-methylated m^{6}A peaks in ccRCC. **Conclusion:** This study presented the first m^{6}A transcriptome-wide map of human ccRCC, which may shed lights on possible mechanisms of m^{6}A-mediated gene expression regulation.

First draft submitted: 3 July 2019; Accepted for publication: 28 November 2019; Published online: 20 December 2019

Keywords: clear cell renal cell carcinoma • m^{6}A-sequencing • modification patterns • N^6-methyladenosine

N^6-Methyladenosine (m^{6}A) is the most prevalent internal mRNA modification in mammalian, and has been reported to play critical roles in gene expression regulation [1]. m^{6}A modification regulates the stability, localization, transportation and translation of target mRNAs in the post-transcriptional level, thus affects various biological processes such as embryo development, self renewal of stem cells, DNA damage response and primary miRNA processing [2–6]. m^{6}A modification is catalyzed by a set of m^{6}A methyltransferases (known as m^{6}A 'writers') such as methyltransferase-like 3 and 14 (METTL3 and METTL14), as well as co-factor, Wilms tumor 1-associated protein (WTAP) [7]. On the other hand, m^{6}A demethylases including fat mass and obesity-associated protein (FTO) and AlkB homolog 5 (ALKBH5, known as m^{6}A 'erasers') can remove methyl radical from RNAs to make m^{6}A modification in a dynamic balance. Another set of m^{6}A-binding proteins (e.g., YT521-B homology domain family YTHDF1/2/3) serve as m^{6}A 'readers' that mediate specific functions of methylated mRNA transcripts [7,8].

As a dynamic process, m^{6}A modification has spatiotemporal properties due to tissue specificity and is in response to internal and external cues. Actually, evidence is emerging that m^{6}A modification is not only associated with the normal biological processes, but also the initiation and progression of different types of cancers [9–12]. With the development of high-throughput assays, it is possible to profile m^{6}A modification pattern on a transcriptome-wide scale. In 2012, two independent studies reported the m^{6}A RNA methylomes in mammalian genomes for the first time by m^{6}A-RNA immunoprecipitation approach followed by high-throughput sequencing (MeRIP-seq) [1,13]. However, the transcriptome-wide distributions of m^{6}A in most kinds of cancers are largely unknown.

Clear cell renal cell carcinoma (ccRCC) is the most common type of kidney cancer, representing approximately 70% of adult renal cell carcinomas, and has profound impact on patients' daily lives [14]. To date, the RNA m^{6}A-methylation profile of ccRCC has not been figured out yet. We report here transcriptome-wide m^{6}A profiling in ccRCC samples and the tumor-adjacent normal tissues for the first time, demonstrating the highly diverse m^{6}A modification patterns between these two groups. Abnormal m^{6}A RNA modifications in ccRCC are proved to modulate gene expressions and cancer-related pathways. We hope this study will facilitate further investigations of potential roles of m^{6}A modification in ccRCC pathogenesis.

Future Medicine

Methods

Patients & samples

The study was approved by the Ethics Committee of the hospital, and the written informed consents were obtained from all the participants. All procedures performed in studies involving human participants were compliant with the ethical standards. ccRCC tissues and tumor-adjacent normal tissues were collected at the time of surgery. Samples were immediately separated into 1.5 ml RNase-free centrifuge tubes and stored at -80°C until RNA isolation. Three pairs of ccRCC group (Ca) and normal control group (NC) samples were selected for RNA sequencing, and the remaining samples were saved for validation (Supplementary Table 1).

High-throughput m^{6}A & mRNA sequencing

Total RNA was harvested from tissue samples and underwent quality control (QC) process using NanoDrop ND-1000 (Thermo Fisher Scientific, MA, USA). High-throughput m^{6}A and mRNA sequencing were performed by Cloudseq Biotech, Inc. (Shanghai, China) according to the published procedure [13] with slight modifications. Briefly, fragmented RNA was incubated with anti-m^{6}A polyclonal antibody (Synaptic Systems, 202003, Goettingen, Germany) in IP, immunoprecipitation buffer at 4°C for 2 h. The mixture was then immunoprecipitated by incubation with protein-A beads (Thermo Fisher Scientific) at 4°C for additional 2 h. Then, bound RNA was eluted from the beads with N^6-methyladenosine (Berry & Associates, PR3732, Dexter, USA) in IP buffer and then extracted with Trizol reagent (Thermo Fisher Scientific) according to the manufacturer's instruction. Purified RNA was used for RNA-seq library generation with NEBNext® Ultra™ RNA Library Prep Kit (New England Biolabs, MA, USA). Both the input sample without immunoprecipitation and the m^{6}A IP samples were subjected to 150 bp paired-end sequencing on Illumina HiSeq sequencer, Illumina, CA, USA. Raw data of RNA-seq and m^{6}A-seq have been uploaded to GEO database (accession number GSE138274, https://www.ncbi.nlm.nih.gov/geo/query/acc.cgi?acc=GSE138274).

Sequencing data analysis

Paired-end reads were harvested from Illumina HiSeq 4000 sequencer, and were quality controlled by Q30. After 3′ adaptor-trimming and low-quality reads removed by cutadapt software (v1.9.3) [15], the high-quality clean reads of all libraries were aligned to the reference genome (UCSC HG19) by Hisat2 software (v2.0.4) [16]. For m^{6}A sequencing, methylated sites on RNAs (m^{6}A peaks) were identified by MACS software [17]. Differentially methylated sites were identified by diffReps [18]. m^{6}A peaks that were overlapping with transcript exons were picked out for further study. For mRNA sequencing, raw counts were get by HTSeq software (v0.9.1), and normalized by edgeR software. Differentially expressed mRNAs were identified by p-value and fold change. Gene ontology [19] and pathway enrichment analysis [20] were performed based on the differentially methylated protein coding genes and differentially expressed mRNAs.

Gene-specific m^{6}A qPCR validation

Seven genes with differentially methylated sites according to m^{6}A-seq were tested by reverse transcription (RT)-qPCR. A portion of fragmented RNA was saved as the input control. The rested RNA was incubated with anti-m^{6}A antibody-coupled beads. The m^{6}A-containing RNAs were then immunoprecipitated and eluted from the beads. Both input control and m^{6}A-IP samples were subjected to RT-qPCR with gene-specific primers.

The following are the gene-specific qPCR primers:

- NPR3: F: 5′ AGGGAGATGCACCGTCAA 3′; R: 5′ CCGGGTGTAAACCTGTGC 3′;
- ANK3: F: 5′ ATGGGAGAGTTCGGGAGC 3′; R: 5′ CCTGGATGGTCCCCTTCT 3′;
- PLOD2: F: 5′ TGGCATGAACACGTCTTTG 3′; R: 5′ TTGGCCCAAAGTGAAGTTG 3′;
- UMOD: F: 5′ TCCACCCCCAAGAAAACA 3′; R: 5′ TACACATTTGCCCCAGGC 3′;
- KLF11: F: 5′ AAGTCTGGTGGCCTGCTG 3′; R: 5′ GAGGGGTGGTTTTCCTGG 3′;
- NXPH4: F: 5′ CTCAGCCGCCAGAGAAGA 3′; R: 5′ ACGGGCCAAAGAGCAAG 3′;
- NDUFA4L2: F: 5′ AGCTAAGTTGGGGTGGGG 3′; R: 5′ TGGCTCCTGCCATATCGT 3′

Statistical analysis

Data from three or more independent experiments were presented as the mean ± standard deviation (SD). Statistical analysis were done using SPSS 22.0 and GraphPad Prism 5.0 softwares. Paired Student's *t*-tests were performed

between cancer and adjacent normal samples. One-way analysis of variance was used to access the differences among three or more groups. Differences with $p < 0.05$ were defined as the threshold for significance.

Results

Transcriptome-wide m^{6}A-Seq revealed global m^{6}A modification patterns in ccRCC

Human ccRCC tissues versus tumor-adjacent normal tissues from three patients were selected for transcriptome-wide m^{6}A-sequencing (m^{6}A-seq) and RNA-sequencing (RNA-seq) assays. In general, 10.8–21.4 million reads were generated from each m^{6}A-seq dataset, and 34.0–39.4 million reads were generated from RNA-seq dataset (also serving as the corresponding m^{6}A-seq input library) (Supplementary Table 2). The percentages of mapped reads were from 70.92 to 79.75%, respectively.

A total of 10,880 m^{6}A peaks were identified by model-based analysis of ChIP-seq (MACS) [17] in Ca group, representing transcripts of 6527 genes. In tumor-adjacent NC group, 8981 m^{6}A peaks were identified, which correspond with transcripts of 5760 genes (Figure 1A & B). The differences and overlaps in m^{6}A RNA between the individuals were shown by Venn diagram in Supplementary Figure 1. Among them, only 3961 individual m^{6}A peaks and 3761 m^{6}A-modified genes were detected within both the groups. When compared with NC group, Ca group had 6919 new peaks appeared with the disappearance of 5020 peaks, indicating the significant difference in global m^{6}A modification patterns between Ca and NC groups (Figure 1A–C).

The m^{6}A methylomes were further mapped by HOMER software. The top consensus motifs in the 15,899 identified m^{6}A peaks were GAACA and GGACA (Figure 1D), which were similar to previous studies [7,21]. By analyzing the distribution of m^{6}A-modified peaks per gene, we found that nearly 40% of all modified genes (3394/8526) had the unique m^{6}A modification peak. The majority of genes (6268/8526) had one to three m^{6}A-modified sites (Figure 1E). In particular, cancer-unique m^{6}A genes tended to have more m^{6}A-modified sites than NC-unique m^{6}A genes (genes with two m^{6}A-modified sites: 23.03 vs 17.66%; genes with three m^{6}A-modified sites: 7.52 vs 4.65%; Figure 1F).

Then, we analyzed the distribution of m^{6}A in the whole transcriptome of Ca and NC samples. Both total and unique m^{6}A peaks from the two groups were analyzed. m^{6}A peaks were divided into transcription starting site region (TSS), 5′UTR, coding sequence (CDS), stop codon and 3′UTR according to their locations in RNA transcripts. In general, the m^{6}A peaks were especially enriched in the vicinity of TSS, CDS and the stop codon (Figure 1G), which was consistent with previous m^{6}A-seq results [1,13]. The Ca-unique m^{6}A peaks showed a distinct pattern from NC-unique peaks, with a relative increase of m^{6}A deposit appeared around TSS region, and a relative decrease in CDS region (Figure 1H & I). These 6919 Ca-unique peaks included 196 peaks from 5′UTR, 3077 from TSS, 1912 from CDS, 976 from stop codon and 758 from 3′UTR region.

Abnormal m^{6}A-modified genes are enriched in cancer-related signaling pathways

The abundance of the m^{6}A peaks between NC and Ca samples were compared. Among the 3961 m^{6}A peaks detected in both the samples, a total of 569 differentially methylated sites were picked for further study. A total of 210 hyper-methylated m^{6}A sites were found in Ca group compared with NC group, and 359 hypo-methylated m^{6}A sites were discovered (fold change >2, $p < 0.05$) (Figure 2A). The remaining m^{6}A peaks were regarded as unchanged m^{6}A peaks. The differentially methylated sites in these two groups showed altered intensity, with the GGACU motif around the corresponding m^{6}A peaks, according to Integrative Genomics Viewer (IGV) software (Figure 2B) [22].

Pathway analysis revealed that hyper- and hypo-methylated m^{6}A sites represented genes in Ca samples were enriched in many pathways involved in kidney biology and cancer pathogenesis, including miRNAs in cancer, TGF-β, Ras and cAMP signaling pathways (Figure 2C & D). Protein interaction network analysis of abnormal m^{6}A-modified genes was performed by Cytoscape software [23]. TGFBR1, EGF and PIK3R1 were the most central proteins (Figure 2E). Therefore, these genes and corresponding signaling pathways were of great importance to the protein–protein interaction network and molecular events in ccRCC. In addition, transcripts which had cancer-unique m^{6}A peaks were also involved in many cancer-related pathways and biological processes, such as cell proliferation, adhesion, migration and DNA repair (Figure 2F & G).

Identification of differentially expressed genes in ccRCC by RNA-seq

In the RNA-seq dataset (m^{6}A-seq input library), we discovered that the global mRNA expression patterns between ccRCC samples and adjacent normal tissues were significantly different. Analysis of mRNA expression profiles

10.2217/epi-2019-0182

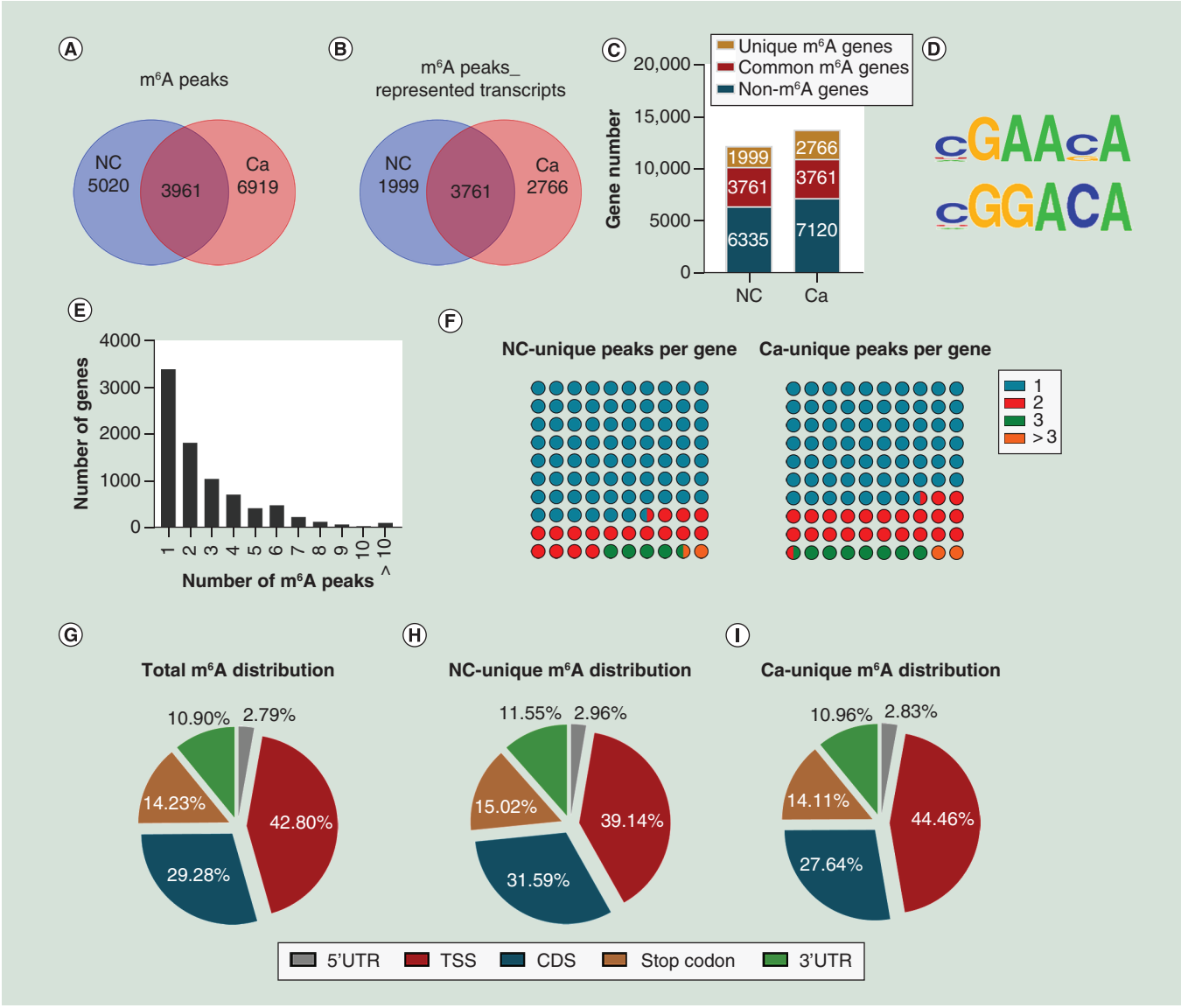

Figure 1. Transcriptome-wide m^{6}A-seq and analysis of m^{6}A peaks. (A) Identification of m^{6}A peaks by model-based analysis of ChIP-seq algorithm. The numbers of cancer-unique, normal-unique and common m^{6}A peaks are shown; **(B)** Venn diagram of m^{6}A peaks-represented transcripts of two groups; **(C)** summary of m^{6}A-modified genes identified in m^{6}A-seq; **(D)** top m^{6}A motifs enriched from all identified m^{6}A peaks; **(E)** the distribution of m^{6}A-modified peaks per gene; **(F)** the distribution of m^{6}A-modified peaks per gene in Ca-unique and NC-unique m^{6}A genes; **(G–I)** the proportion of m^{6}A peak distribution in the indicated regions in NC and Ca samples (G); and the loss of existing m^{6}A peaks (NC-unique peaks, H) or appearance of new m^{6}A peaks (Ca-unique peaks, I) in Ca group.
Ca: Clear cell renal cell carcinoma group; NC: Normal control group.

showed that 1327 mRNAs were significantly dysregulated versus controls, including 886 up-regulated mRNAs and 441 down-regulated mRNAs (fold change >2, $p < 0.05$). The scatter plot and the hierarchical clustering of the RNA-seq data were shown in Figure 3A & B.

The differentially expressed genes were selected for ingenuity gene ontology and pathway analysis. It revealed that abnormal up-regulated genes in Ca samples were significantly enriched in biological processes involving cellular stress response, oxidative stress-induced cell death and immunity (Figure 3C), which was consistent with the cancer pathology. Moreover, pathway analysis showed that HIF-1 signaling pathway, tight junction and metabolism pathways were significantly altered in ccRCC Ca samples (Figure 3D & E).

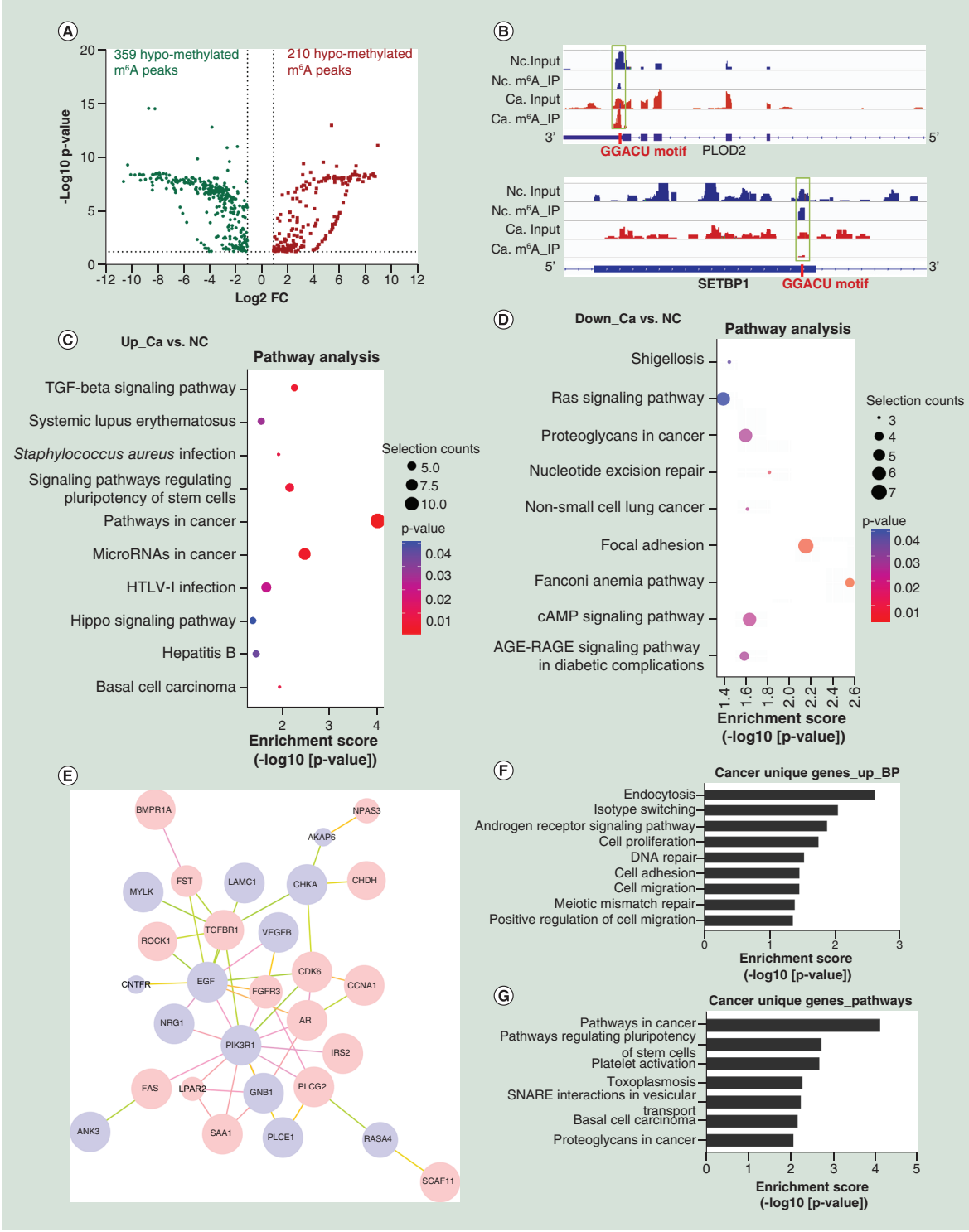

Figure 2. Global m^{6}A modification changes in clear cell renal cell carcinoma (ccRCC) tissues compared with tumor-adjacent normal tissues. (A) Identification of 210 hyper-methylated and 359 hypo-methylated m^{6}A peaks, which displayed a significant increase or decrease (fold change >2, $p < 0.05$), respectively, in abundance in Ca samples compared with NC samples. **(B)** The m^{6}A abundances in PLOD2 and SETBP1 mRNA transcripts in NC and Ca samples, as detected by m^{6}A-seq. The m^{6}A peaks shown in the green rectangles are those that have a significant increased or reduced abundance (fold change >2, $p < 0.05$) in Ca samples compared with NC samples. **(C)** Gene set enrichment pathway analysis of transcripts with increased m^{6}A modification in Ca samples compared with NC samples by topGO. **(D)** Pathway analysis of transcripts with reduced m^{6}A modification in Ca samples compared with NC samples. **(E)** Graph of the protein interaction network of abnormal m^{6}A-modified genes conducted by Cytoscape. The interaction network was constructed from identified proteins according to their m^{6}A modification status in clear cell renal cell carcinoma samples compared with NC samples. Red and violet circles represent the induced and reduced m^{6}A modification of genes, respectively. **(F)** Gene ontology analysis of biological process of transcripts with cancer-unique m^{6}A peaks conducted by topGO. **(G)** Pathway analysis of transcripts with cancer-unique m^{6}A peaks. Ca: Clear cell renal cell carcinoma group; NC: Normal control group.

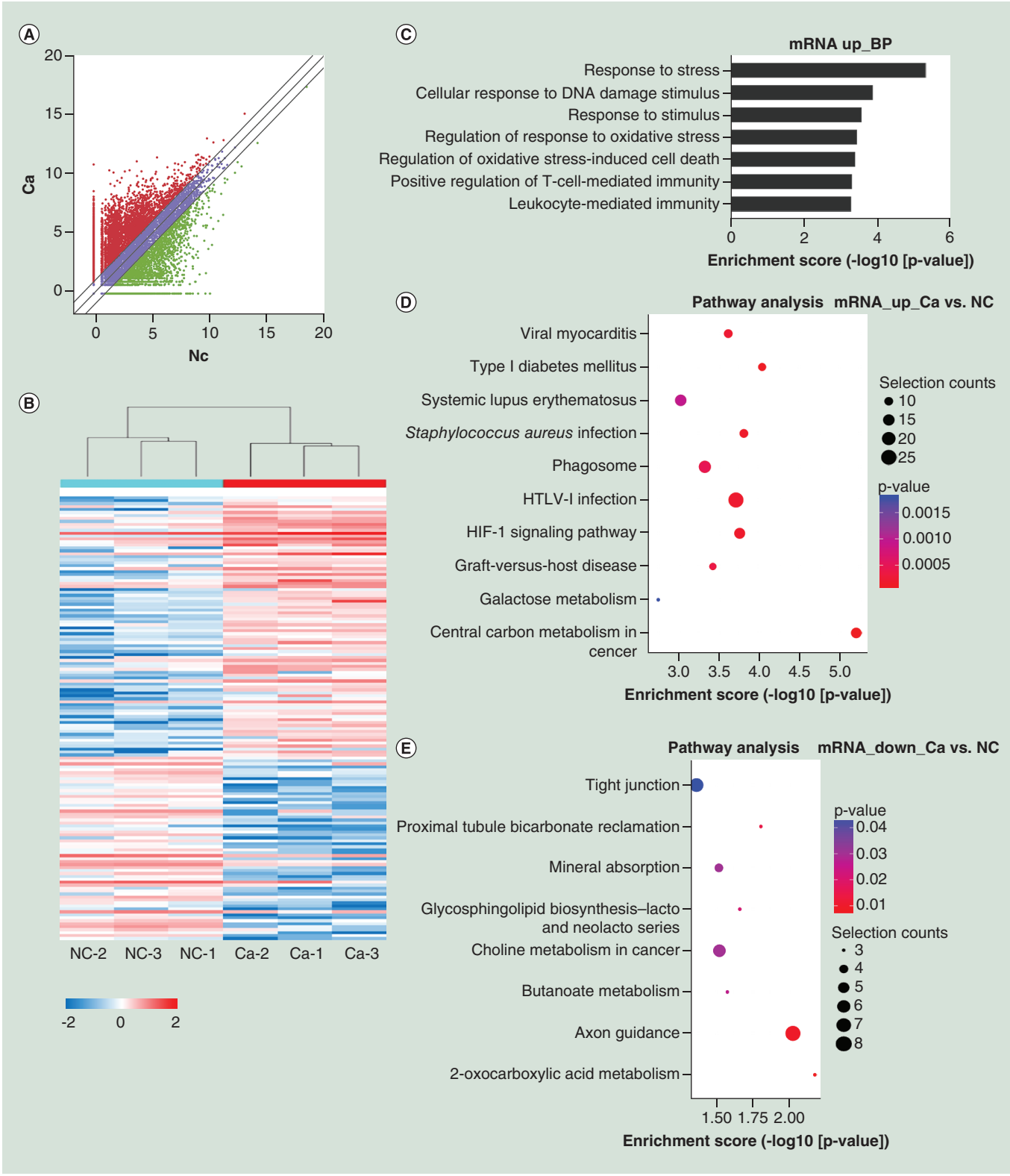

Figure 3. Identification of differentially expressed genes in RCC by RNA-seq. (A) The scatter plot of the RNA-seq data. **(B)** Heat map of RNA-seq data of Ca samples and adjacent normal tissues. Rows: mRNAs; columns: normal control group and Ca samples. Red, white and blue indicate the upregulation, unchanged expression and downregulation of mRNAs, respectively. **(C)** Gene ontology analysis of biological process involved in upregulated genes in Ca samples conducted by topGO. **(D)** Pathway analysis of 886 upregulated genes in Ca samples. **(E)** Pathway analysis of 441 downregulated genes in Ca samples.
Ca: Clear cell renal cell carcinoma group.

Conjoint analysis of m^{6}A- RNA binding protein immunoprecipitation (RIP)-seq & RNA-seq data of ccRCC & normal samples

By cross-analysis of the m^{6}A-Seq and RNA-seq data, we discovered a positive correlation of differentially methylated m^{6}A peaks and gene expression level in Ca samples and adjacent normal tissues (Figure 4A). In 210 hyper-methylated m^{6}A sites detected by m^{6}A-Seq, we found ten targets with up-regulated mRNA transcripts (fold change >2, $p < 0.05$), namely 'hyper-up'. Four genes were found to have hyper-methylated m^{6}A sites along with down-regulated mRNA transcripts (fold change >2, $p < 0.05$), namely 'hyper-down'. In the contrast, ten of 359 genes with hypo-methylated m^{6}A sites showed up-regulated mRNA transcripts (fold change >2, $p < 0.05$), namely 'hypo-up', and 11 of 359 genes with hypo-methylated m^{6}A sites showed down-regulated mRNA transcripts (fold change >2, $p < 0.05$), namely 'hypo-down' (Figure 4B & C). Genes that exhibited a significant change in both m^{6}A level and mRNA transcript abundance in ccRCC samples compared with normal controls were listed in Table 1. Notably, 73% (11/15) of the down-regulated mRNA transcripts were associated with hypo-methylated m^{6}A peaks in ccRCC samples. Meanwhile, the numbers of 'hyper-up' and 'hypo-down' genes were more than those of 'hyper-down' and 'hypo-up' genes, with larger fold changes and smaller p-values (Figure 4B & Table 1). It indicated that m^{6}A modifications tend to have a positive correlation of mRNA expression in ccRCC.

We were wondering whether the location of m^{6}A peaks in RNA transcripts, or the number of m^{6}A peaks per transcripts was associated with gene expression levels. Figure 4D displayed the overall expression levels of m^{6}A-methylated and non-m^{6}A-methylated transcripts in different groups. RNA transcripts were then divided into subgroups according to their m^{6}A modification sites. All m^{6}A peaks, NC-unique peaks and Ca-unique peaks were analyzed. As a result, RNA transcripts with m^{6}A modifications around the stop codon tended to have reduced gene expression levels compared with those of 5′UTR or CDS modifications (Figure 4E). As shown in Figure 1E, different genes have different numbers of m^{6}A-modified sites. By analyzing the relative expression levels of these genes, we found that more m^{6}A-modified sites per gene were associated with the elevated gene expression. Genes with more than six m^{6}A-modified sites tended to have more mRNA abundance compared with the ones with unique m^{6}A modification peak (Figure 4F). Since gene expressions are controlled by complex factors, the impact of differential m^{6}A modifications on gene expressions is worth further investigation.

To examine the relationship of genes listed in Table 1 and ccRCC in a large cohort, we used Gene Expression Profiling Interactive Analysis (GEPIA) [24], a software based on the cancer genome atlas (TCGA) database, for further analysis. Seven of these genes associated with ccRCC (NDUFA4L2, PLOD2, NXPH4, KLF11, NPR3, UMOD and ANK3) were picked out for further study. Among these, NDUFA4L2, NXPH4 and PLOD2 had elevated expressions in the large cohort of ccRCC patients (n = 523) compared with normal controls (n = 100) (Supplementary Figure 2A–C). ANK3 and UMOD had reduced expressions in ccRCC patients (Supplementary Figure 2D & E). In addition, levels of PLOD2 and ANK3 changed continuously with disease severity (Supplementary Figure 2F & G). Different expression levels of PLOD2, ANK3, KLF11, NPR3 and UMOD also had profound impact on overall survival rate of ccRCC patients. It showed that high PLOD2 expression level was associated with lower overall survival of ccRCC patients (Supplementary Figure 2H). Decreased expression levels of ANK3, KLF11, NPR3 and UMOD were associated with lower overall survival of ccRCC patients (Supplementary Figure 2I–L).

To further confirm the results of our m^{6}A-seq data, we conducted gene-specific m^{6}A qPCR assays for several hyper-methylated and hypo-methylated genes (NDUFA4L2, PLOD2, NXPH4, KLF11, NPR3, UMOD and ANK3). We observed the same m^{6}A-level changes in six out of the seven genes (85.7%; Figure 5A), demonstrating the reliability of our transcriptome-wide m^{6}A-seq data. Sequentially, mRNA levels of above-mentioned genes were measured in 17 pairs of NC and Ca samples (Figure 5B). Results showed a similar tendency of m^{6}A-methylated level and mRNA expressions.

Finally, global m^{6}A levels of NC and Ca samples were measured by LC–MS/MS. Ca samples exhibited relatively higher total m^{6}A levels than tumor-adjacent samples (Figure 5C). It demonstrated that ccRCC samples had unique m^{6}A modification patterns that are diverse from normal tissues, both in transcriptome-wide and gene-specific scales.

Discussion

As the most abundant internal modification in eukaryotic mRNAs, m^{6}A methylation was reported to play critical roles not only in various normal biological processes, but also the initiation, progression and even drug responses of cancers [8]. Nevertheless, the transcriptome-wide distributions of m^{6}A modification in most kinds of cancers, and the specific role of abnormal m^{6}A modifications in cancer pathogenesis are largely unknown. In this study, we

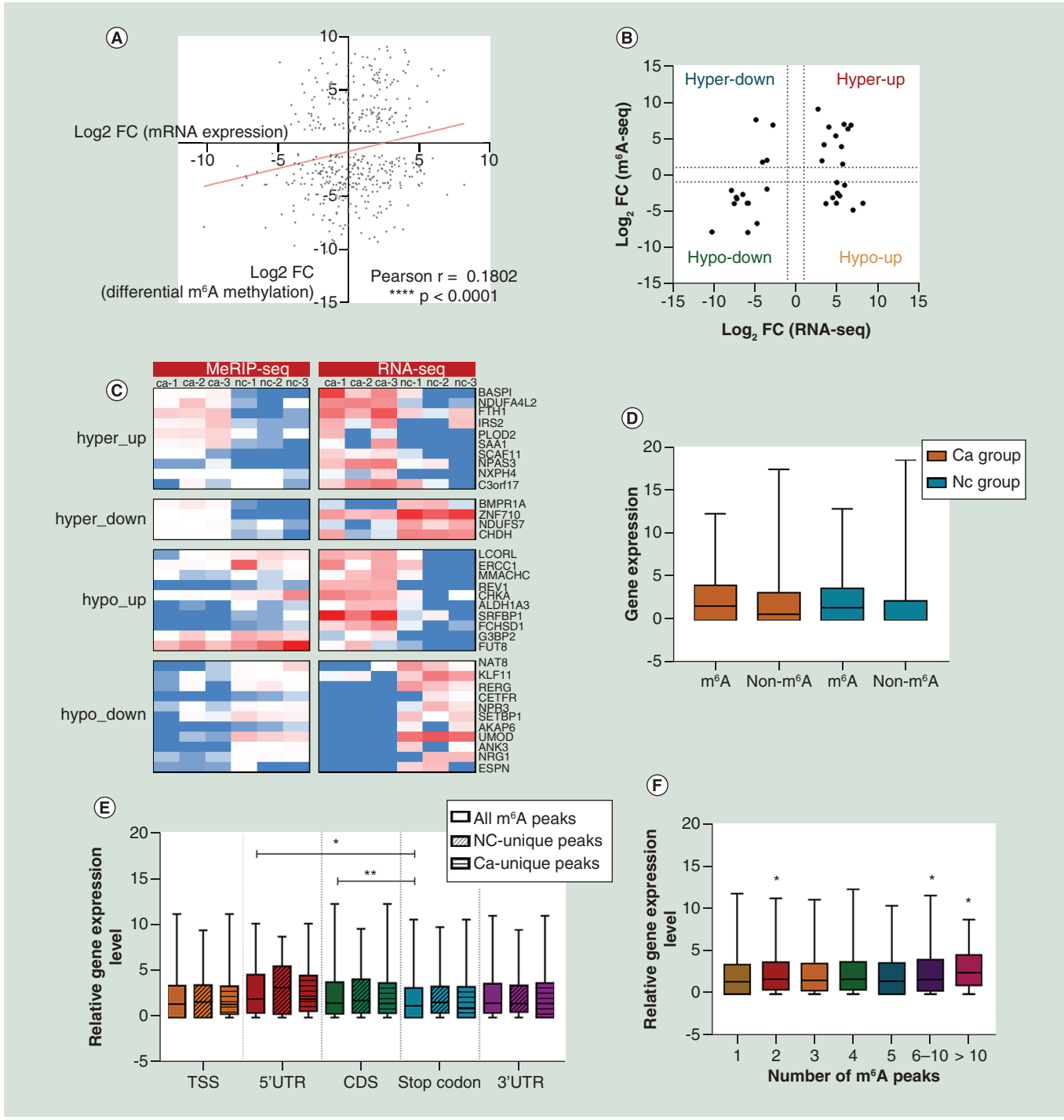

Figure 4. Conjoint analysis of m^{6}A-RIP-seq and RNA-seq data. (A) Dot plot of Log2 fold change (FC) (mRNA expression) against Log2 FC (differential m6A methylation) showing a positive correlation between overall m^{6}A methylation and mRNA expression level (Pearson r = 0.1802; $p < 0.0001$). **(B)** Distribution of genes with a significant change in both m^{6}A and mRNA levels in clear cell renal cell carcinoma group samples compared with adjacent normal tissues (fold change >2, $p < 0.05$). **(C)** Heat map of 'hyper-up', 'hyper-down', 'hypo-up' and 'hypo-down' genes represented in (B). **(D)** The overall expression levels of m^{6}A-methylated and non-m^{6}A-methylated transcripts in different groups. **(E)** The location of m^{6}A peaks in RNA transcripts and relative gene expression level in all m^{6}A peaks, normal control group-unique peaks and clear cell renal cell carcinoma group-unique peaks. *$p < 0.05$; **$p < 0.01$ compared with 'stop codon' region. **(F)** Relative mRNA expression levels of transcripts containing different number of m^{6}A peaks. *$p < 0.05$ compared with the first column (m^{6}A peak = 1).

Table 1. List of 35 genes that exhibit a significant change in both m^{6}A level and mRNA transcript abundance in clear cell renal cell carcinoma samples compared with normal controls.

Gene name	Pattern	Chromosome	m^{6}A level change					mRNA level change		
			Peak region	Peak start	Peak end	Fold change	p-value	Strand	Fold change	p-value
FTH1	Hyper-up	chr11	3′UTR	61,731,961	61,732,180	522.2449	7.06E-12	-	6.6230	0.0114
BASP1	Hyper-up	chr5	stopC	17,275,961	17,276,160	122.4857	7.47E-09	+	59.2580	1.65E-05
SAA1	Hyper-up	chr11	TSS	18,287,720	18,287,843	113.9900	1.42E-08	+	107.5578	0.0064
IRS2	Hyper-up	chr13	stopC	11,040,7681	11,040,8060	94.7423	2.15E-08	-	16.4770	0.0222
NDUFA4L2	Hyper-up	chr12	CDS	57,630,811	57,631,100	79.5341	2.50E-08	-	82.3201	2.57E-05
SCAF11	Hyper-up	chr12	TSS	46,328,229	46,328,293	41.0000	0.0007	-	29.3065	0.0365
NPAS3	Hyper-up	chr14	CDS	33,525,110	33,525,200	17.6000	0.0308	+	11.0253	0.0126
PLOD2	Hyper-up	chr3	stopC	14,578,8101	145,788,460	14.5422	2.18E-09	-	47.7402	0.0351
C3orf17	Hyper-up	chr3	stopC	11,272,4061	112,724,260	3.7468	0.0262	-	9.2541	0.0486
NXPH4	Hyper-up	chr12	TSS	57,610,577	57,610,760	2.7366	0.0011	+	53.1164	0.0239
ANK3	Hypo-down	chr10	CDS	61,831,801	61,832,360	0.0040	2.64E-09	-	0.0175	0.0327
UMOD	Hypo-down	chr16	TSS	20,364,010	20,364,200	0.0042	7.10E-09	-	0.0009	2.50E-09
NAT8	Hypo-down	chr2	TSS	73,869,444	73,869,537	0.0094	1.16E-08	-	0.0384	0.0266
NRG1	Hypo-down	chr8	stopC	32,621,541	32,621,920	0.0627	1.34E-08	+	0.0056	0.0043
CNTFR	Hypo-down	chr9	CDS	34,590,079	34,590,120	0.0658	0.0444	-	0.0168	0.0401
AKAP6	Hypo-down	chr14	CDS	33,290,607	33,290,760	0.0658	0.0444	+	0.0183	0.0382
NPR3	Hypo-down	chr5	TSS	32,711,437	32,711,700	0.1004	7.97E-09	+	0.0070	0.0036
SETBP1	Hypo-down	chr18	CDS	42,532,861	42,533,305	0.1144	1.05E-07	+	0.0067	0.0022
ESPN	Hypo-down	chr1	TSS	6,484,847	6,485,020	0.1501	0.0022	+	0.0116	0.0139
RERG	Hypo-down	chr12	TSS	15,290,763	15,290,920	0.2219	0.0126	-	0.0044	0.0003
KLF11	Hypo-down	chr2	CDS	10,188,061	10,188,320	0.2492	0.0028	+	0.0890	0.0138
SRFBP1	Hypo-up	chr5	CDS	12,135,6041	121,356,300	0.0341	0.0037	+	126.9226	1.75E-07
CHKA	Hypo-up	chr11	stopC	67,820,981	67,821,380	0.0626	2.14E-07	-	12.8577	0.0079
REV1	Hypo-up	chr2	TSS	10,010,6278	100,106,360	0.0649	0.0444	-	291.6240	9.99E-05
FCHSD1	Hypo-up	chr5	CDS	14,103,0601	141,030,684	0.0658	0.0444	-	31.0071	0.0059
ERCC1	Hypo-up	chr19	TSS	45,981,993	45,982,086	0.1108	5.61E-07	-	22.7624	0.0103
LCORL	Hypo-up	chr4	stopC	17,885,381	17,885,920	0.1326	7.03E-08	-	41.2087	0.0052
ALDH1A3	Hypo-up	chr15	TSS	10,141,9896	101,419,980	0.1587	0.0194	+	35.2600	0.0293
MMACHC	Hypo-up	chr1	TSS	45,965,921	45,966,085	0.1721	2.00E-07	+	33.7842	0.0299
G3BP2	Hypo-up	chr4	stopC	76,570,121	76,570,600	0.3650	0.0398	-	62.3844	0.0203
FUT8	Hypo-up	chr14	stopC	66,209,221	66,209,780	0.4707	0.0008	+	32.4381	0.0376
BMPR1A	Hyper-down	chr10	stopC	88,683,381	88,683,780	189.5143	9.99E-09	+	0.0352	0.0180
ZNF710	Hyper-down	chr15	TSS	90,545,717	90,545,784	114.1000	1.16E-08	+	0.1463	0.0043
CHDH	Hyper-down	chr3	3′UTR	53,850,323	53,850,460	3.9571	0.0039	-	0.0883	0.0090
NDUFS7	Hyper-down	chr19	TSS	1,383,706	1,383,900	3.3162	0.0169	+	0.0606	0.0118

CDS: Coding sequence; TSS: Transcription starting site region.

illustrated global m^{6}A modification patterns in ccRCC samples versus tumor-adjacent normal tissues, analyzing gene expression and cancer-related pathways modulated by abnormal m^{6}A RNA modifications.

We figured out that m^{6}A modification pattern in ccRCC samples was distinct from that of normal controls, with a higher total m^{6}A level and 1899 more m^{6}A peaks identified in Ca group. By analyzing the differently methylated transcripts and cancer-unique m^{6}A peaks, cancer-related biological process and pathways were significantly enriched, indicating the relationship between abnormal m^{6}A modifications and ccRCC pathogenesis. Such global change of m^{6}A modification profiles could result from the abnormal expression of key m^{6}A enzymes. However, the expression levels of key components of m^{6}A writers, erasers and readers remained unchanged according to our mRNA-seq data (Supplementary Table 3). This may be due to the limited sample size in the present study. Subsequent studies of larger sample size are needed to investigate the reason of global m^{6}A change in ccRCC.

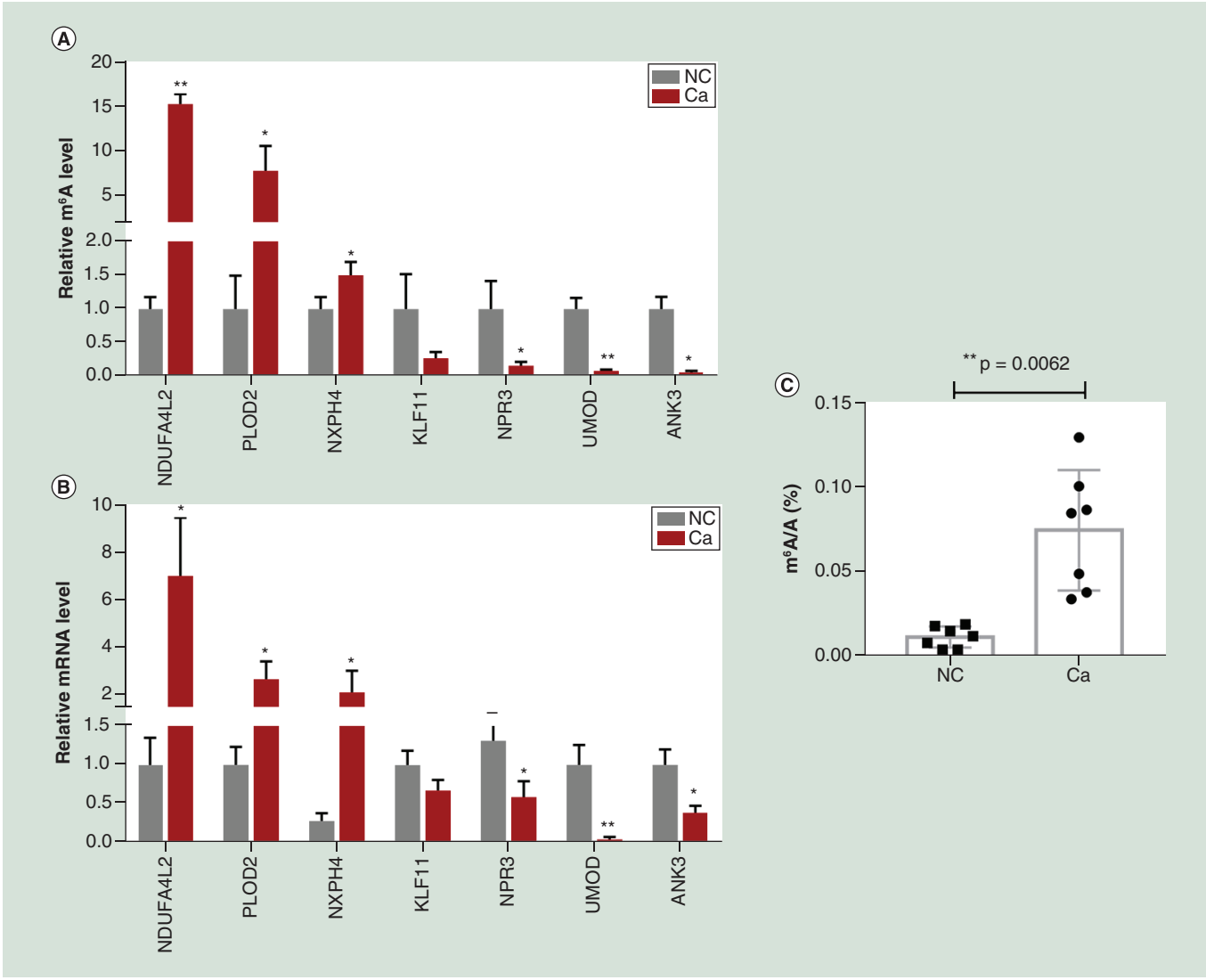

Figure 5. Gene-specific m^{6}A qPCR assays and detection of global m^{6}A levels. (A) Gene-specific m^{6}A qPCR validation of m^{6}A level changes of seven representative hyper-methylated or hypo-methylated genes in normal control group and clear cell renal cell carcinoma group samples. **(B)** Relative mRNA levels of seven representative genes were measured by real-time PCR in normal control group and clear cell renal cell carcinoma group samples. **(C)** m^{6}A/A ratio of polyA-RNAs isolated from normal control group and clear cell renal cell carcinoma group samples were measured by LC–MS/MS. The bar shows the mean from n = 7 technical replicates.

Combined analysis of our m^{6}A-seq and mRNA-seq data revealed 35 genes in Ca group, which have differently methylated m^{6}A sites along with significant changes of mRNA abundance compared with NC group (fold change >2, $p < 0.05$, Table 1). These genes may play critical roles in the development of ccRCC and are worth further investigation. By GEPIA database analysis, NDUFA4L2, PLOD2, NXPH4, KLF11, NPR3, UMOD and ANK3 were discovered to be associated with ccRCC in the large cohort. Different expression levels of PLOD2, ANK3, KLF11, NPR3 and UMOD also had profound impact on the survival rate of ccRCC patients (Supplementary Figure 2). Moreover, some of the genes were reported to facilitate tumor growth and metastasis in different kinds of cancers. For instance, PLOD2 was reported to promote proliferation, migration and invasion of glioma via PI3K/Akt signaling [25]. NDUFA4L2 was related to ccRCC malignancy and was regulated by ELK1 [26]. ANK3 expression was associated with androgen receptor stability, which may affect the prognosis of prostate cancer patients and breast cancer patients [27,28]. BASP1 was involved in acute myeloid leukemia [29] and cervical cancer [30]. Thus, further functional studies may help to clarify the molecular mechanisms of above-mentioned genes in the

development of ccRCC. Moreover, modulating m^{6}A modifications could become a strategy to treat human diseases in the future.

In the present study, when pictured in a global scale, m^{6}A modifications tend to have positive correlation with mRNA expression in ccRCC samples (Figure 4A). This result was further confirmed by gene-specific m^{6}A qPCR assays and mRNA qPCR analysis (Figure 5A & B). This observation was different from some previous studies [3,31], but consistent with others [12,32]. It may be due to the differences in disease status and sample collection. Moreover, the specific role of m^{6}A methylation upon gene expression largely depends on the function of downstream m^{6}A 'readers' [7,8]. In the present study, only cytoplasm mRNA level was measured. It was reported that m^{6}A modification could influence the stability, localization, transportation and translation of target mRNAs that depend on the recognition of different kinds of 'readers'. In addition, functional experiments are needed to further confirm the regulatory role of m^{6}A RNA modifications upon gene expression in ccRCC. Knocking down or overexpression key enzymes of m^{6}A modifications can become good strategies to investigate m^{6}A methylation-mediated cellular responses.

Conclusion

This study presented the first m^{6}A transcriptome-wide map of human ccRCC. It provided a potential link between abnormal m^{6}A RNA modifications and cancer-related gene expressions. We hope it can be a starting roadmap for discovering m^{6}A functions, and shed some light on further studies regarding m^{6}A modifications in ccRCC.

Future perspective

This study presented the first m^{6}A transcriptome-wide map of human ccRCC, and identified differentially expressed mRNA transcripts with hyper-methylated or hypo-methylated m^{6}A modifications. This may help to further investigate the mechanisms of m^{6}A-mediated gene expression regulation. New therapeutic strategies of ccRCC by modulating m^{6}A-methylated transcripts or m^{6}A-related genes may be developed.

Summary points

- m^{6}A RNA modification in clear cell renal cell carcinoma (ccRCC) samples is highly diverse from that of normal controls, with cancer-unique m^{6}A peaks and altered peak enrichment regions.
- There are 6919 new m^{6}A peaks appeared with the disappearance of 5020 peaks in ccRCC samples compared with normal control group samples.
- The unique distribution pattern of m^{6}A in ccRCC is associated with cancer-related pathways.
- We identified 14 hyper-methylated m^{6}A peaks in mRNA transcripts that were significantly upregulated (10; hyper-up) or downregulated (4; hyper-down), and 21 hypo-methylated m^{6}A peaks in mRNA transcripts that were significantly upregulated (10; hypo-up) or downregulated (11; hypo-down).
- We identified a positive correlation of m^{6}A RNA modifications upon gene expression in ccRCC samples.

Supplementary data

To view the supplementary data that accompany this paper please visit the journal website at: www.futuremedicine.com/doi/suppl/10.2217/epi-2019-0182

Author contributions

D Xue and X He designed and supervised the whole study. Y Chen performed experiments, provided statistical analysis and wrote the manuscript. C Zhou and Y Sun collected samples and clinical data, and revised the manuscript. D Xue gave final approval of the version to be published.

Acknowledgments

The authors thank the patients who contributed to this study. They thank Cloudseq Biotech, Inc. (Shanghai, China) for the m^{6}A meRIP sequencing service and bioinformatics support.

Financial & competing interests disclosure

This project was supported by Jiangsu Provincial 333 Department Support project (BRA2017116) and Changzhou Municipal Science and Technology Bureau Support project (CE20175030). The authors have no other relevant affiliations or financial involvement

with any organization or entity with a financial interest in or financial conflict with the subject matter or materials discussed in the manuscript apart from those disclosed.

No writing assistance was utilized in the production of this manuscript.

Ethical conduct of research

The study was approved by the ethics committee of the hospital, and the written informed consent was obtained from all participants. All procedures performed in studies involving human participants were compliant with the ethical standards.

References

Papers of special note have been highlighted as: • of interest; •• of considerable interest

1. Dominissini D, Moshitch-Moshkovitz S, Schwartz S *et al.* Topology of the human and mouse m6A RNA methylomes revealed by m6A-seq. *Nature* 485(7397), 201–206 (2012).

•• **Publishes a novel approach, N^6-methyladenosine (m^6A)-seq, and reveals transcriptome-wide m^6A RNA methylomes and the distribution patterns in human and mouse.**

2. Wang Y, Li Y, Toth JI, Petroski MD, Zhang Z, Zhao JC. N6-methyladenosine modification destabilizes developmental regulators in embryonic stem cells. *Nat. Cell Biol.* 16(2), 191–198 (2014).
3. Wang X, Lu Z, Gomez A *et al.* N6-methyladenosine-dependent regulation of messenger RNA stability. *Nature* 505(7481), 117–120 (2014).
4. Wang X, Zhao BS, Roundtree IA *et al.* N(6)-methyladenosine modulates messenger RNA translation efficiency. *Cell* 161(6), 1388–1399 (2015).
5. Alarcon CR, Lee H, Goodarzi H, Halberg N, Tavazoie SF. N6-methyladenosine marks primary microRNAs for processing. *Nature* 519(7544), 482–485 (2015).
6. Xiang Y, Laurent B, Hsu CH *et al.* RNA m(6)A methylation regulates the ultraviolet-induced DNA damage response. *Nature* 543(7646), 573–576 (2017).
7. Fu Y, Dominissini D, Rechavi G, He C. Gene expression regulation mediated through reversible m(6)A RNA methylation. *Nat. Rev. Genet.* 15(5), 293–306 (2014).

• **Reviews the crucial function of gene expression regulation mediated by reversible m^6A RNA methylation.**

8. Deng X, Su R, Weng H, Huang H, Li Z, Chen J. RNA N(6)-methyladenosine modification in cancers: current status and perspectives. *Cell Res.* 28(5), 507–517 (2018).

• **Reviews the important functions of m^6A modification in cancer pathogenesis.**

9. Liu J, Eckert MA, Harada BT *et al.* m(6)A mRNA methylation regulates AKT activity to promote the proliferation and tumorigenicity of endometrial cancer. *Nat. Cell Biol.* 20(9), 1074–1083 (2018).
10. Chen M, Wei L, Law CT *et al.* RNA N6-methyladenosine methyltransferase-like 3 promotes liver cancer progression through YTHDF2-dependent posttranscriptional silencing of SOCS2. *Hepatology* 67(6), 2254–2270 (2018).
11. Zhang S, Zhao BS, Zhou A *et al.* m(6)A demethylase ALKBH5 maintains tumorigenicity of glioblastoma stem-like cells by sustaining FOXM1 expression and cell proliferation program. *Cancer cell* 31(4), 591.e6–606.e6 (2017).
12. Li Z, Weng H, Su R *et al.* FTO plays an oncogenic role in acute myeloid leukemia as a N(6)-methyladenosine RNA demethylase. *Cancer Cell* 31(1), 127–141 (2017).
13. Meyer KD, Saletore Y, Zumbo P, Elemento O, Mason CE, Jaffrey SR. Comprehensive analysis of mRNA methylation reveals enrichment in 3′ UTRs and near stop codons. *Cell* 149(7), 1635–1646 (2012).

•• **Reports the novel method for transcriptome-wide m^6A localization, MeRIP-seq, and revealed the distribution pattern of m^6A.**

14. Frew IJ, Moch H. A clearer view of the molecular complexity of clear cell renal cell carcinoma. *Annu. Rev. Pathol.* 10, 263–289 (2015).
15. Martin M. Cutadapt removes adapter sequences from high-throughput sequencing reads. *EMBnet. J.* 17(1), 10–12 (2011).
16. Kim D, Langmead B, Salzberg SL. HISAT: a fast spliced aligner with low memory requirements. *Nat. Methods* 12(4), 357–360 (2015).
17. Zhang Y, Liu T, Meyer CA *et al.* Model-based analysis of ChIP-Seq (MACS). *Genome Biol.* 9(9), R137 (2008).
18. Shen L, Shao NY, Liu X, Maze I, Feng J, Nestler EJ. diffReps: detecting differential chromatin modification sites from ChIP-seq data with biological replicates. *PLoS ONE* 8(6), e65598 (2013).
19. Alexa A, Rahnenführer J. Gene set enrichment analysis with topGO (2009). https://bioconductor.org/packages/release/bioc/vignettes/topGO/inst/doc/topGO.pdf
20. Tian L, Greenberg SA, Kong SW, Altschuler J, Kohane IS, Park PJ. Discovering statistically significant pathways in expression profiling studies. *Proc. Natl Acad. Sci. USA* 102(38), 13544–13549 (2005).
21. Chen T, Hao YJ, Zhang Y *et al.* m(6)A RNA methylation is regulated by microRNAs and promotes reprogramming to pluripotency. *Cell Stem Cell* 16(3), 289–301 (2015).

22. Thorvaldsdottir H, Robinson JT, Mesirov JP. Integrative Genomics Viewer (IGV): high-performance genomics data visualization and exploration. *Brief. Bioinform.* 14(2), 178–192 (2013).

23. Shannon P, Markiel A, Ozier O *et al.* Cytoscape: a software environment for integrated models of biomolecular interaction networks. *Genome Res.* 13(11), 2498–2504 (2003).

24. Tang Z, Li C, Kang B, Gao G, Li C, Zhang Z. GEPIA: a web server for cancer and normal gene expression profiling and interactive analyses. *Nucleic Acids Res.* 45(W1), W98–W102 (2017).

25. Song Y, Zheng S, Wang J *et al.* Hypoxia-induced PLOD2 promotes proliferation, migration and invasion via PI3K/Akt signaling in glioma. *Oncotarget* 8(26), 41947–41962 (2017).

- **Reports the potential role of *PLOD2* gene in cancer pathogenesis.**

26. Wang L, Peng Z, Wang K *et al.* NDUFA4L2 is associated with clear cell renal cell carcinoma malignancy and is regulated by ELK1. *PeerJ* 5, e4065 (2017).

- **Reports the association of NDUFA4L2 with clear cell renal cell carcinoma.**

27. Wang T, Abou-Ouf H, Hegazy SA *et al.* Ankyrin G expression is associated with androgen receptor stability, invasiveness, and lethal outcome in prostate cancer patients. *J. Mol. Med.* 94(12), 1411–1422 (2016).

28. Kurozumi S, Joseph C, Raafat S *et al.* Utility of ankyrin 3 as a prognostic marker in androgen-receptor-positive breast cancer. *Breast Cancer Res. Treat.* 176(1), 63–73 (2019).

29. Zhou L, Fu L, Lv N *et al.* Methylation-associated silencing of BASP1 contributes to leukemogenesis in t(8;21) acute myeloid leukemia. *Exp. Mol. Med.* 50(4), 44 (2018).

30. Tang H, Wang Y, Zhang B *et al.* High brain acid soluble protein 1(BASP1) is a poor prognostic factor for cervical cancer and promotes tumor growth. *Cancer Cell Int.* 17, 97 (2017).

31. Schwartz S, Mumbach MR, Jovanovic M *et al.* Perturbation of m6A writers reveals two distinct classes of mRNA methylation at internal and 5′ sites. *Cell Rep.* 8(1), 284–296 (2014).

32. Luo GZ, Macqueen A, Zheng G *et al.* Unique features of the m6A methylome in *Arabidopsis thaliana*. *Nat. Commun.* 5, 5630 (2014).